Heat flow studies for large temperature gradients by molecular dynamics simulation

András Baranyai*
Department of Chemical Engineering, University of Tennessee, 419 Dougherty Engineering Building, Knoxville, Tennessee 37996-2200
(Received 1 July 1996)

We derived a molecular dynamics algorithm capable of simulating heat flow in fluids beyond the linear regime. Unlike the synthetic Evans method, our algorithm establishes real temperature differences between two regions of the model system by pumping heat continuously into the high-temperature region and taking it away from the low-temperature region. Since there is no solid phase present, the generated density variation is small. The heat flow can be calculated from the energy input and output of the thermostat or can be measured by the method of planes. We performed extensive calculations to study the performance of the algorithm and compared the determined heat conductivity coefficients to results obtained by the synthetic method. For the studied simple fluid model the conductivity was found practically independent of the size of the temperature gradient. [S1063-651X(96)11112-0]

PACS number(s): 02.70.−c, 44.10.+i, 05.60.+w, 66.60.+a

I. INTRODUCTION

Thermal conductivity has proven to be one of the most difficult transport coefficients to calculate [1]. Unlike the case of self-diffusion, the heat flux vector is a collective property of the particles [2], which makes the Green-Kubo–type equilibrium calculations much more expensive [3]. In realistic nonequilibrium molecular dynamics (NEMD) simulations the symmetry of the process does not fit as conveniently into the usual periodic boundary conditions as that of shear flow. Thus, it was a breakthrough when Evans [4] and, independently, Gillan and Dixon [5] derived a nonequilibrium molecular dynamics algorithm capable of calculating heat conductivity coefficients. In the Evans algorithm a synthetic external field generated the heat flow. The equations of motion are momentum preserving, homogeneous, and compatible with the usual periodic boundary conditions. ''Warmer'' particles are driven with the field, ''colder'' particles are driven against the field. Linear response theory was used to prove that this heat flux is trivially related to the magnitude of the heat flux induced by a real temperature gradient [4]. The zero field limit value of the heat conductivity can be determined by extrapolating several coefficients obtained at finite external fields.

This extrapolation can be replaced by the subtraction technique [6], which applies external fields several orders of magnitude smaller than those used in NEMD simulations. In the subtraction method the response induced by the perturbing field is computed as the difference between the energy current measured along two trajectories starting from the same point in phase space. The first trajectory is followed by the system under the impact of the small external field while the second trajectory represents an equilibrium state of the system. For a short time the noise along the two trajectories will be highly correlated [7]. Unfortunately, the length of this time is often not sufficient to reach a well-defined plateau of the generated current because Lyapunov instability drives the two trajectories apart in phase space and gradually destroys the excellent noise cancellation.

The synthetic algorithm has been extended to rigid-body molecules by Evans and Murad [8], and subsequently generalized to molecules with arbitrary internal degrees of freedom by Daivis and Evans [9]. All versions of the Evans algorithm use synthetic thermostats, i.e., a feedback mechanism which removes the generated dissipative heat instantaneously in order to maintain a steady state. The presence of the thermostat does not influence the results in the zero field limit [1]. The calculated heat conductivity coefficients, however, have no justification beyond the linear regime. Observed details of the behavior of the model at finite external fields have only questionable relevance to the behavior of real fluids.

If we want to devise an algorithm which is capable of calculating heat conductivity coefficients beyond the linear regime we must return to a more realistic picture of heat flow. There are two early works published in the literature that attempted to calculate heat conductivities in this way. Ashurst [10] placed the fluid between two ''fluid walls'' kept at different temperatures at opposite boundaries of the molecular dynamics box. In the second calculation, performed by Tenebaum *et al.* [11], two stochastic walls were devised which reflected back the particles with random velocities corresponding to the required temperatures. An obvious disadvantage of the second approach is that solid walls introduce large inhomogeneities into the fluid. The structure of the fluid close to the wall is markedly different from that in the bulk.

In the following we devise an algorithm which is a version of the fluid wall approach. The fluid wall is formed from the very same particles as the rest of the system. There is no constraint on the diffusive motion of particles; they can attend every region of the entire system. This conceptually simple algorithm is completely deterministic. The presented model calculations refer to a simple fluid but extension of the method to molecular fluids is straightforward. In Sec. II we describe the basic ideas of our method and present the equations of motion. In Sec. III we give technical details of our calculations. In Sec. IV we present the results and compare

*Present address: Laboratory of Theoretical Chemistry, Eötvös University, H-1518 Budapest 112, Pf.32., Hungary.

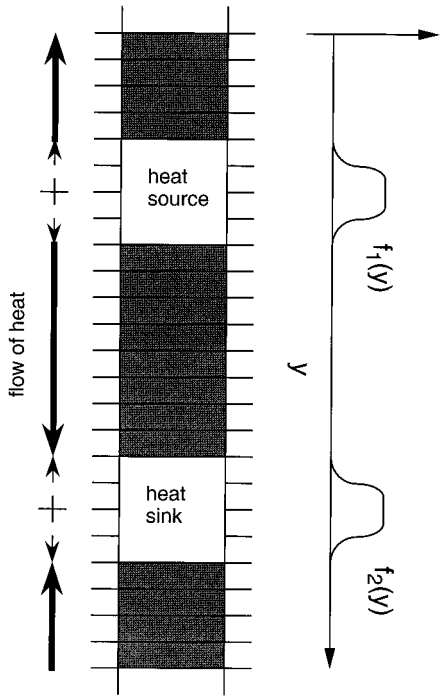

FIG. 1. Two-dimensional projection of our simulation box. Horizontal lines represent the planes through which the heat flow was measured. The white regions are the reservoirs. The schematic pictures of the $f_1(y)$ and $f_2(y)$ weight functions are shown on the right-hand side. The direction of the heat flow is shown on the left-hand side.

the calculated heat conductivities and other system properties to results obtained by the synthetic method. In Sec. V we discuss and conclude this study.

II. THE MOLECULAR DYNAMICS ALGORITHM

To generate a steady heat flow we need a cold reservoir and a hot reservoir incorporated into our system with different but constant temperatures. The best way of achieving this is to use a synthetic thermostatting scheme. Synthetic thermostats ensure that the equations of motion will remain reversible, the heating or cooling will be instantaneous, and the heat transfer will be measurable.

The first systematic approach to perform molecular dynamics calculations at controlled temperature rather than energy was done independently by Hoover *et al.* [12] and Evans [13]. These authors devised a differential feedback scheme which kept the total kinetic energy of the system constant. Now this procedure is referred to as Gaussian thermostat because the form of the equations of motion can be derived from Gauss's principle of least constraint [14]. Shortly after the Gaussian scheme Nosé formulated a thermostat [15] which is formally an integral feedback [16], and for ergodic, equilibrium systems the states are selected from the canonical distribution. For our present purpose the Gaussian scheme is better than the Nosé-Hoover method because for small systems the fluctuations of the random kinetic energy are very large.

In Fig. 1 we show a two-dimensional projection of our simulation box. The system has translational periodicity in every direction. The hot and the cold regions which are under the impact of synthetic thermostats are represented by white squares. In the dark areas only Newton's equations govern the motion of the particles. To maintain periodicity there are two connecting regions between the heated and cooled parts. Thus, we obtain averages of two independent measurements.

Our system is continuous; particles can wander in and out of each part of the elongated simulation box. We do not interfere with this motion but keep track of each particle at every instant because the positions of particles determine whether they belong to a reservoir or to the Newtonian (thermostat-free) region. At the boundaries of the reservoirs this diffusive motion can cause discontinuity. The form of the equations of motion for a particle changes if this particle crosses one of these four possible, imaginary boundaries. To handle this problem we introduced a weight function $f(y)$ (see Fig. 1). This function is zero everywhere in the simulation box except in the thermostatted regions. The shape of the function is arbitrary within the following requirements: $f(y)$ must (i) be zero at the thermostatted region boundaries, (ii) be symmetric with respect to the halving plane of the thermostatted region, (iii) have continuous first derivatives everywhere, and (iv) be as simple as possible. We can use this function to define the equations of motions for the system as follows:

$$\dot{\mathbf{q}}_i = \mathbf{p}_i/m, \qquad \dot{\mathbf{p}}_i = \mathbf{F}_i - f_\beta(y_i)[\kappa_\beta \mathbf{j} + \alpha_\beta \mathbf{p}_i], \tag{1}$$

$\mathbf{q}_i$, $\mathbf{p}_i$, and $\mathbf{F}_i$ are the position, the momentum, and the interparticle force of particle i, and m is the particle mass. The unit vector of the y axis, $\mathbf{j}$, is parallel with the direction of the temperature gradient. Subscript $\beta = 1,2$ distinguishes between the hot and the cold parts of the system. The two functions $f_1(y)$ and $f_2(y)$ have identical shapes but the first is different from zero only in the hot reservoir region while the second has nonzero values only in the cold reservoir region (see Fig. 1). The thermostatting multiplier α_β is multiplied with the $f_\beta(y)$ function. Since outside the reservoir regions this function is zero the rest of the particles are not effected by the thermostat.

We also use the weight function to define the temperature inside the reservoirs.

$$T_\beta = \frac{\Sigma_{i=1}^{N} f_\beta(y_i)\mathbf{p}_i^2}{3km\Sigma_{i=1}^{N} f_\beta(y_i)}, \tag{2}$$

where k is Boltzmann's constant.

The role of $f(y)$ is clear from Eq. (2). Let the value of this function vary between unity and zero. If it is unity the particle belongs completely to the reservoir region *at this instant*. If it is zero the particle is not influenced directly by the feedback scheme at this time. For intermediate cases the particle is part of the transitional wall region which separates the reservoir from the Newtonian regime. This construction of the wall ensures that the temperature of the reservoir changes continuously when a particle enters or leaves the region.

We introduced another multiplier κ into the momentum equation of (1). This is necessary in order to fix the y momenta of the reservoir regions because Eq. (1) does not preserve the total momentum of the system. Although the discrepancy per time step is negligible without continuous correction it might accumulate considerably. We experienced that after a short initial period the whole system started to flow in one direction. This flow is undesirable for two reasons. First, it destroys the symmetry of the system. The two thermostat-free regions will no longer be equivalent. Second, the collective shift of particles out of the reservoir regions distorts the measured heat input-output. The temperature of the cold reservoir appears to be warmer because the whole region is shifted away relative to the coordinate frame of the simulation box. Similarly, the temperature of the hot reservoir appears to be cooler. To prevent this, we defined the collective y momentum for both reservoirs as follows:

$$P_{y\beta}=\frac{\Sigma_{i=1}^{N} f_\beta(y_i) p_{yi}}{\Sigma_{i=1}^{N} f_\beta(y_i)}. \tag{3}$$

This definition is completely analogous to the definition of the temperature in Eq. (2). The determination of the multipliers κ and α follows the usual procedure [1]. From $\dot{T}_\beta=0$ and $\dot{P}_{y\beta}=0$ using Eq. (1) the solution for the multipliers is as follows:

$$\alpha=\frac{F(C+D-E)-A(H+J-I)}{BF-2A^2},$$
$$\kappa=\frac{-2A(C+D-E)+B(H+J-I)}{BF-2A^2}, \tag{4}$$

where the capital letters represent the following sums:

$$A=2\sum p_{yi} f^2(y_i), \quad B=2\sum \mathbf{p}_i^2 f^2(y_i),$$
$$C=2\sum \mathbf{F}_i \mathbf{p}_i f(y_i),$$
$$D=\sum \mathbf{p}_i^2 \dot{f}(y_i), \quad E=3T\sum \dot{f}(y_i),$$
$$F=\sum f^2(y_i), \quad H=\sum F_{yi} f(y_i), \quad I=P_y\sum \dot{f}(y_i),$$
$$J=\sum p_{yi} \dot{f}(y_i).$$

There are two multiplier sets for the two identical $f(y)$ functions but for the sake of simplicity the β subscripts are omitted from Eq. (4). All sums run from 1 to N. Furthermore,

$$\dot{f}(y_i)=\left.\frac{df}{dy}\right|_{y=y_i} \frac{p_{yi}}{m}. \tag{5}$$

The energy input-output is the time derivative of the Hamiltonian. From Eq. (1) it is simply

$$\frac{dH}{dt}=\sum_{i=1}^{N} [(\partial H/\partial \mathbf{q}_i)\dot{\mathbf{q}}_i+(\partial H/\partial \mathbf{p}_i)\dot{\mathbf{p}}_i]=-\alpha\sum_{i=1}^{N} \frac{\mathbf{p}_i^2}{m} f(y_i). \tag{6}$$

From Eq. (6) we omitted the contribution of κ because in steady states it was by several orders of magnitude smaller than the contribution of α.

After some initial period the evolution of the system governed by Eqs. (1) and (4) will reach a steady state. The amount of random kinetic energy taken away by the cooler will be equal with the energy provided by the heater. Since we have two connecting regions, we may expect the amount of heat passing through the $y-z$ area of our box in the Newtonian part to be the average of these two energy terms. Unfortunately, this is true only approximately because there is a nonzero heat flux in the reservoir regions as well. The behavior of the whole system will be effected by our choice of $f(y)$. The shape and width of $f(y)$ will influence the results.

To understand the role of $f(y)$ we are using another, completely independent method which measures the heat flux directly. This method was developed quite recently by Todd *et al.* [17,18], as a simple and general statistical mechanical technique for calculating the heat flux vector and the pressure tensor of atomistic, nonequilibrium fluids. The method, termed the method of planes (MOP), is devised for fluids being *inhomogeneous* in one direction. The corresponding expressions of the Irving-Kirkwood procedure are only approximations for such systems. The planes can be located anywhere in the system but their normals must be parallel with the direction of the inhomogeneity, in our case, the y axis. The horizontal black lines of Fig. 1 represent our choice of planes. This work can also serve as the first independent check of the MOP technique.

III. TECHNICAL DETAILS OF THE CALCULATION

Our model system contained $8\times256=2048$ WCA particles. The WCA interaction is a spherically symmetric pair-potential given by the following equation:

$$\phi(r)=\begin{cases} 4\epsilon[(\sigma/r)^{12}-(\sigma/r)^6]+\epsilon, & r<2^{1/6}\sigma \\ 0, & r\geqslant 2^{1/6}\sigma. \end{cases} \tag{7}$$

Reduced units are used throughout the paper, for which ϵ,σ and the atomic mass m are unity. The overall reduced density ρ was 0.8. An advantage of the WCA interaction is that at these parameters the distance between two adjacent planes (1.71) is larger than the interaction range of the pair-potential. This can be utilized during the calculations for time saving purposes.

Our choice of $f(y)$ was uniform plateau $[f(y)=1]$ smoothly connected to zero by the following cubic polynomial:

$$f(y)=a(y-y_0)^3+b(y-y_0)+0.5, \tag{8}$$

where a and b are constants determined from the required properties of $f(y)$ and the actual value of y_0.

It is well known that methods using differential feedback accumulate numerical errors gradually drifting the value of

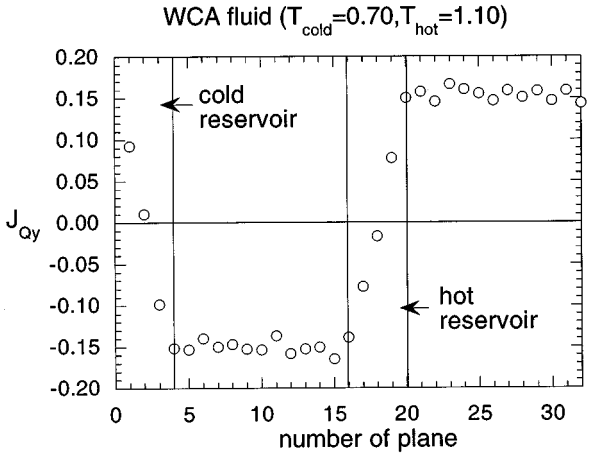

FIG. 2. The measured heat fluxes for the $\delta T = 0.40$ system.

the fixed variable. There are two ways to correct it. The constrained variable can be rescaled after every few hundred time steps or one can supplement the integrator with a proportional feedback which corrects the numerical errors continuously [19]. In the case of the reservoir temperatures we used proportional feedback while rescaling proved to be more suitable for correcting the constrained momenta of the reservoirs.

We performed calculations with five different reservoir temperature pairs. In each case the median temperature was chosen to be 0.9. The results are averages of steady state runs of 600 000 time steps. The reduced time step was 0.002, half of the usual value and a fifth-order Gear algorithm integrated the equations of motion. This accuracy was necessary to reduce the role of ''numerical dissipation.'' The contribution of the proportional feedback and momentum rescaling to the energy transfer of the thermostats was negligible, several orders of magnitude smaller than that coming from α. The remaining average y momenta of the fluid slabs (particles between two adjacent planes) were very small, a random distribution of values of 10^{-4}–10^{-5}. With respect to the MOP technique we provide no details, the reader is referred to Refs. [17] and [18].

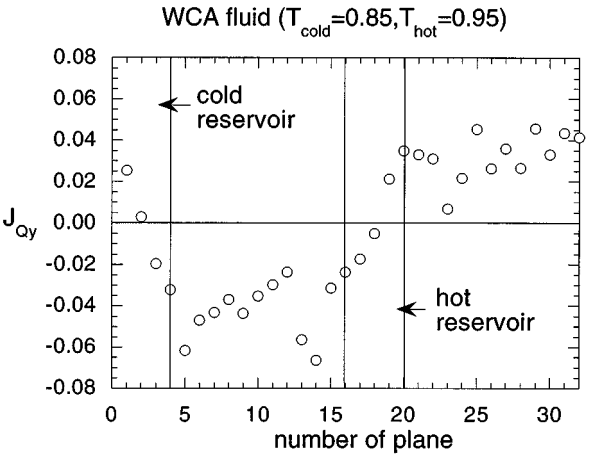

FIG. 3. The measured heat fluxes for the $\delta T = 0.10$ system.

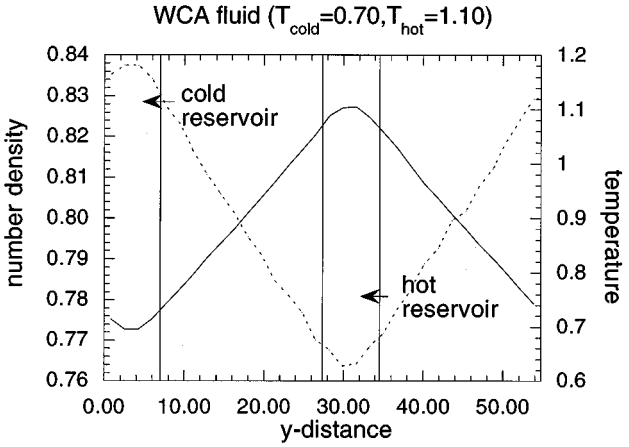

FIG. 4. The density and temperature variation in the fluid as functions of the y distance ($\delta T = 0.40$). The solid line is the temperature; the dotted line is the number density.

IV. RESULTS OF THE CALCULATION

We present two sets of figures to show the most important features of the simulated system. The first set refers to the case when the temperature difference between the two reservoirs was the largest, $\delta T = 0.40$. In the second case the reservoir temperature difference in $\delta T = 0.10$. This is the second smallest temperature difference in these calculations. Figures 2 and 3 show the heat flow vectors calculated by the MOP method. In steady states, outside the reservoir regions the heat flux must be constant. This is reproduced quite well in the case of the large temperature gradient (Fig. 2). The impact of the random noise, however, is visible in the small field case (Fig. 3).

Figures 4 and 5 show the distribution of the number density and temperature in the simulation box in terms of the reduced distance along the y axis. The density and temperature values are averages of slabs defined by two adjacent planes. Both the temperature and the density are basically linear outside the reservoirs, although in the case of small temperature gradients, the relative fluctuations can be significant.

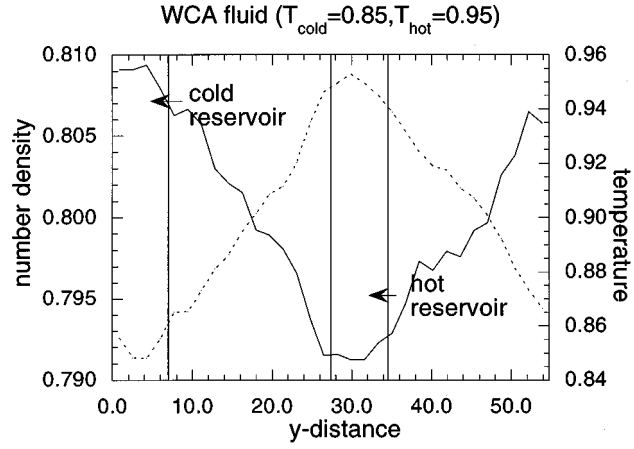

FIG. 5. The density and temperature variation in the fluid as functions of the y distance ($\delta T = 0.40$). The solid line is the temperature; the dotted line is the number density.

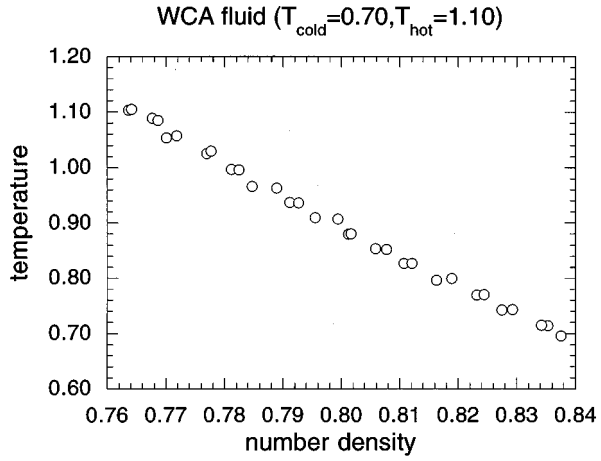

FIG. 6. Temperature in terms of the density ($\delta T = 0.40$). Reservoir data are also shown.

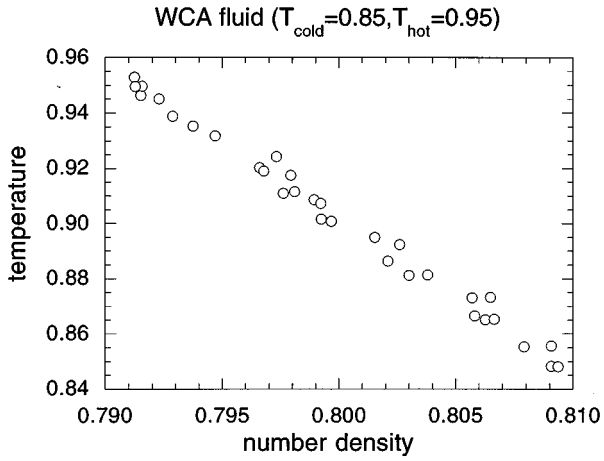

FIG. 7. Temperature in terms of the density ($\delta T = 0.10$). Reservoir data are also shown.

In Figs. 6 and 7 we show the temperature in terms of the number density. After the previous figures it is not surprising that these functions are also linear. Within the accuracy of our calculations there is no difference between these curves in the studied temperature gradient range. The $T = f(\rho)$ curves fit onto the same linear line. The only difference is that they occupy shorter or longer lengths of this line according to their temperature and density ranges.

We also studied the directional distribution of the random kinetic energy. We found that for these temperature gradients there is no difference between the kinetic temperatures of the x, y, and z directions in the model.

The heat conductivities calculated from the MOP heat flux averages are shown in Table I. Since, within the errors of the calculations, the temperature gradients and the heat flux vectors in the thermostat-free regions were constant, we simply took the average of the heat flux vectors measured at planes outside the reservoirs, and divided it by the average temperature gradient of the same region. The use of the actual temperature values produced slightly different $\delta T/\Delta T$ ratios. Not surprisingly, uncertainties in the heat conductivity coefficients were much larger at smaller temperature gradients.

In Table II we show the amount of heat per unit time provided or removed by the thermostat [see Eq. (6)]. If we use these data the calculated heat conductivity coefficients will be much larger than the values of Table I. The cause of this discrepancy is that certain amount of the heat is dissipated in the reservoir itself. There is an unpreventable heat flow in these regions too (see Figs. 2 and 3). In order to remove this distorting effect from our calculations we extrapolated our results to the hypothetical reservoir of zero width along the y axis. For three systems ($\delta T = 0.40, 0.30, 0.20$) we performed the same calculations with rescaled $f(y)$ functions. The functions had the same shape as before but their width was only half of the previous value. The heat transfer and the calculated heat conductivity coefficients decreased substantially. Using these two heat conductivity values for extrapolation we could determine the ''zero-width'' coefficients. The extrapolated coefficients were in agreement with the values calculated with the help of the MOP method.

The idea of the infinitely thin reservoir layer is conceptually identical with the stochastic wall of Tenebaum *et al.* [11]. However, in our case there is no solid wall with its induced extra inhomogeneity and no need for complicated kinetic recipes. Certainly, the extrapolation means more calculations but the simplicity of the method is attractive. The described method with extrapolation can be used for any molecular model. (At present the MOP technique exists only for atomic particles [17,18].)

Performing calculations with different system sizes and time steps we studied the accuracy of the heat transfer measurement. There are several factors to be optimally chosen to obtain the best results by the extrapolation scheme.

If the temperature gradient is very small ($\Delta T < 0.005$) the uncertainty in the heat transfer calculation becomes significant. For very large gradients ($\Delta T > 0.025$) the amount of heat going through the fluid is so high that we have to de-

TABLE I. Heat conductivity results calculated as the ratio of the MOP heat flux average (pot, potential contribution; kin, kinetic contribution) and the temperature gradient average in the thermostat-free region. The numbers in parentheses indicate the uncertainty in units of the last decimal digit: 6.10(8) means 6.10 ± 0.08.

δT	0.40	0.30	0.20	0.10	0.05
ΔT	0.0250	0.0186	0.0127	0.062	0.0035
J_{Qy} (pot)	0.085	0.062	0.042	0.019	0.011
J_{Qy} (kin)	0.068	0.051	0.036	0.018	0.010
λ	6.10(8)	6.07(10)	6.13(14)	6.04(30)	5.94(40)

TABLE II. Heat conductivity results calculated from the energy input-output of the thermostat. [$\lambda=(dQ/dt)(1/AR)$ where $AR=46.78$ is the cross section area of our box and dQ/dt is the average of the heat input and output; the h subscript refers to calculations with the half-sized reservoirs; λ_{ext} is the extrapolated value.] Uncertainty in λ_{ext} is ± 0.40.

δT	0.40	0.30	0.20	0.10	0.05
dQ/dt (in)	9.38	6.78	4.74	2.04	1.10
dQ/dt (out)	9.20	6.81	4.66	2.17	1.14
λ	7.93	7.81	7.93		
$dQ/dt\ (\text{in})_h$	8.18	6.15	4.24		
$dQ/dt\ (\text{out})_h$	8.50	6.05	4.30		
λ_h	7.05	7.00	7.09		
λ_{ext}	6.17	6.19	6.25		

crease the time step to prevent intolerable inaccuracy. In addition to the time-step reduction, the inhomogeneity will also be undesirably high, which may render the slab averages meaningless. (In such cases the intervention of the feedback term in the dynamics of the reservoir particles will also be unnecessarily strong, although we want their behavior as close to the Newtonian dynamics as possible.)

The size of the thermostat region has also an optimum. If the ratio of the reservoir/Newtonian particles is very small we face the previous problems (time-step reduction, etc.) of large temperature gradients. Nevertheless, we should not have big reservoirs because we want to extrapolate to the zero width of this region. There is no need to employ too many reservoir particles from the point of view of the economy of the calculations either, because their role is merely to facilitate the heat transfer.

In Fig. 8 we show the extrapolation of heat conductivity coefficients calculated by the Evans method at $T=0.9$ and $\rho=0.8$ for 500 WCA particles. Each point is the average of half a million time steps ($\Delta t=0.004$). These state variables characterize the middle layer in our inhomogeneous system. The accuracy of the Evans method is very good in its usual range of external fields ($F=0.1-0.4$). However, these fields are an order of magnitude larger than the corresponding temperature gradients in our calculations [1]. Actually, the error bars of the two low-field calculations by the synthetic method are much bigger than the uncertainties in the λ-s calculated by our method. Our largest temperature gradients ($\Delta T=0.025-0.0186$) are close to the smallest ($TF=0.018$) external field value (see Table I). [The errors in the results (transformed always into λ values) were calculated by dividing each simulation run into 10 blocks. The error bars correspond to one standard deviation of the block averages.]

The extrapolated zero field value of Fig. 8 is 5.92 (we omitted the two low field λ-s from the extrapolation because of their large uncertainties). The value of 5.92 permits a slight field dependence of the heat conductivity coefficient, although this is within the range of the uncertainties. The possible increase of the conductivity with increasing temperature gradients does not contradict to the qualitative picture of the Evans method. The minimal overlap in the typical range of external fields studied by the two methods, however, prevents us from drawing a definite conclusion in this respect.

The temperature gradients of our calculations are very high. If we convert the reduced units by identifying our simple spherically symmetric particles with liquid argon the reported temperature gradients correspond to 10^7-10^8 K/cm. Then it is not surprising that we can observe density variations within our simulation box. These variations are absent from the synthetic method, although the fields typically used in such calculations are larger by an order of magnitude than ours. If one is interested only in heat conductivity coefficients in the linear regime the homogeneity of the synthetic method is an advantage because it permits the use of much smaller systems. However, the synthetic method creates an artificial system which has no relevance to real fluids beyond the linear regime. Details of the system dynamics, the structure of the nonequilibrium liquid cannot be studied by using the synthetic method. For instance, in our calculations the distribution of the random kinetic energy in the x, y, and z directions is absolutely uniform despite the inhomogeneities of the density. This not true for the synthetic method at its *typical* external fields. At $F=0.3$ the kinetic temperature in the flow direction is 0.942 while in the perpendicular directions it is only 0.879. Details of the thermostatting scheme play an important role in the synthetic method. (To obtain the results of Fig. 8 we applied the standard Gaussian thermostat with the usual $-\alpha\mathbf{p}$ term.) A further noticeable difference is that in our method the kinetic contribution to the heat flux calculated by the MOP method is 40–50 % of the total. This is considerably smaller in the synthetic method, 14–16 %.

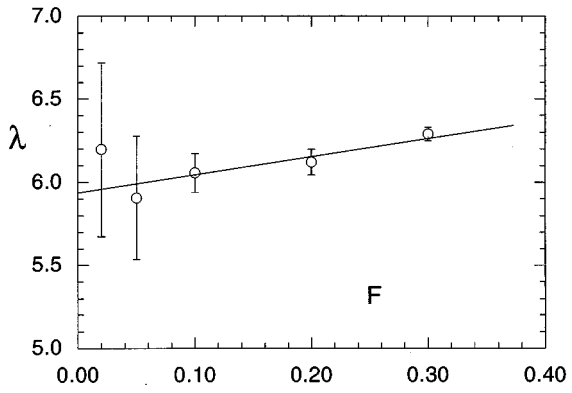

FIG. 8. Heat conductivity coefficients as determined by the synthetic method at different external fields ($N=500$, $T=0.9$, and $\rho=0.8$).

V. CONCLUSIONS

We devised a method to determine the thermal conductivity coefficients of fluids beyond the linear regime. The method is simple and easily applicable to any molecular model used at present in computer simulations.

For the model of atomistic particles we had two different ways of calculating the coefficients. First we used the recently developed MOP technique, which has an excellent performance; its accuracy is comparable to that of the Irving-Kirkwood expressions of homogeneous systems. The MOP results served as cross checks for the trivial extrapolation method when the heat flow is measured with the amount of heat pumped into and out of the system by the thermostats. Although the latter method requires more runs with several different reservoir widths, it needs no direct heat flux calculations. This simplicity makes it very attractive for complex molecular systems.

If one is interested only in values of thermal conductivity coefficients of simple, equilibrium fluids the homogeneous and synthetic method of Evans serves better because much smaller system size can be used with reasonable accuracy. However, it is also clear that the artificial homogeneity of the synthetic method tells us nothing about the structural details of the steady state system and the behavior of the thermal conductivity coefficient beyond the linear regime.

The results of the Evans method refer to a well-defined state point of the fluid. In our case there is a continuous variation of temperature and number density in the simulation box. However, variations of system properties can be monitored. Temperature, temperature gradient, and pressure can be calculated along the long axis of the simulation box. In this way we can measure the thermal conductivity coefficients for a range of state points of the fluid in a single simulation. This compensates us for the more time-consuming calculations in our bigger system. A further advantage of our algorithm is that the properties of our system, in contrast to the synthetic method, are not influenced by the choice of the synthetic thermostats because only Newton's equations of motion govern the dynamics of the particles. The only reasonable requirement of our method is to limit the energy input or output per particle in order to keep the dynamics of the reservoir region close to that of the Newtonian region.

As an example we studied the heat conductivity of simple soft spherical particles. In the case of this model system we experienced no substantial dependence of the coefficient on the size of the temperature gradient. Even the temperature variations in terms of the number density were practically linear in the range studied. These results can serve as a reference for more complex molecular systems.

ACKNOWLEDGMENTS

The author gratefully acknowledges support through a NSF Grant No. CTS-9101326 to Professor Peter T. Cummings.

[1] D. J. Evans and G. P. Morris, *Statistical Mechanics of Nonequilibrium Liquids* (Academic, New York, 1990).
[2] M. P. Allen and A. J. Masters, Mol. Phys. **79**, 435 (1993).
[3] D. Levesque, L. Verlet, and J. Kürkijärvi, Phys. Rev. A **7**, 1690 (1983).
[4] D. J. Evans, Phys. Lett. A **91**, 457 (1982).
[5] M. J. Gillan and M. Dixon, J. Phys. C **16**, 869 (1983).
[6] C. Massobrio and G. Ciccotti, Phys. Rev. A **30**, 3191 (1984).
[7] G. Cicotti, G. Jacucci, and I. R. McDonald, J. Stat. Phys. **21**, 1 (1979).
[8] D. J. Evans and S. Murad, Mol. Phys. **68**, 1219 (1989).
[9] P. J. Daivis and D. J. Evans, Mol. Phys. **81**, 1289 (1994).
[10] W. T. Ashurst, in *Advances in Thermal Conductivity* (University of Missouri–Rolla, Rolla, 1976).
[11] A. Tenenbaum, G. Ciccotti, and R. Gallico, Phys. Rev. A **25**, 2778 (1982).
[12] W. G. Hoover, A. J. C. Ladd, and B. Moran, Phys. Rev. Lett. **48**, 1818 (1982).
[13] D. J. Evans, J. Chem. Phys. **78**, 3297 (1983).
[14] D. J. Evans, W. G. Hoover, B. H. Failor, B. Moran, and A. J. C. Ladd, Phys. Rev. A **8**, 1016 (1983).
[15] S. Nosé, J. Chem. Phys. **81**, 511 (1984).
[16] W. G. Hoover, Phys. Rev. A **31**, 1695 (1985).
[17] B. D. Todd, P. J. Daivis, and D. J. Evans, Phys. Rev. E **51**, 4362 (1995).
[18] B. D. Todd, D. J. Evans, and P. J. Daivis, Phys. Rev. E **52**, 1627 (1995).
[19] A. Baranyai and D. J. Evans, Mol. Phys. **70**, 53 (1990).